UNIVERSITY OF CALIFORNIA SAN DIEGO

Low-Molecular-Weight Protein Tyrosine Phosphatase Promotes Prostate Cancer Progression

A Thesis submitted in satisfaction of the requirements
for the degree Master of Science

in

Biology

by

Joseph Chang

Committee in charge:

Professor Stephanie Stanford, Chair
Professor Jens Lykke-Andersen, Co-chair
Professor Enfu Hui

2019

The Thesis of Joseph Chang is approved, and it is acceptable in quality and form for publication on microfilm and electronically:

Co-Chair

Chair

University of California San Diego

2019

DEDICATION

In recognition of Dr. Stephanie Stanford in her organization and support of the laboratory, constant attention to the progress of science, and training as a scientist.

In recognition of Redeemer's Grace Church and its members who have provided comfort, love, joy, and mutual encouragement in the Lord.

In recognition of my parents and their loving care, generous protection, and unwavering support for over two decades.

In recognition of God our Father, who dwells in inaccessible light, who sustains me by His providential grace. To Him be all the glory, both now and forevermore!

TABLE OF CONTENTS

LIST OF ABBREVIATIONS

PCa	Prostate cancer
LMPTP	Low molecular weight protein tyrosine phosphatase
GSK-3β	Glycogen synthase kinase 3β
PTK	Protein tyrosine kinase
PTP	Protein tyrosine phosphatase
PDGFRA	Platelet derived growth factor receptor alpha
IR	Insulin receptor
EphA2R	Ephrin A2 receptor
AR	Androgen receptor
TCGA	The Cancer Genome Atlas
DMEM	Dulbecco's Modified Eagle media
FBS	Fetal bovine serum
I.U.	International units
RNA	Ribonucleic acid
DNA	Deoxyribonucleic acid
gDNA	Genomic DNA
PCR	Polymerase chain reaction
CRISPR/Cas9	Clustered regularly interspaced short palindromic repeats, Cas9 technology
qPCR	quantitative PCR
RT	Reverse transcriptase
PMSF	Phenylmethylsulfonyl fluoride
BCA	Bicinchoninic acid assay
SDS-PAGE	Sodium dodecyl sulfate-polyacrylamide gel electrophoresis
TBS-T	Tris-buffered saline with Tween 20
HRP	Horseradish peroxidase
GFP	Green fluorescent protein
LB	Lysogeny broth

FACS	Fluorescence-activated cell sorting
HEPES	4-(2-hydroxyethyl)-1-piperazineethanesulfonic acid
EDTA	Ethylenediamine tetraacetic acid
PBS	Phosphate buffered saline
KO	Knockout
RT	Room temperature
C.B. 17 SCID	Severe combined immunodeficiency spontaneous mutation PRKDC
UV	Ultraviolet
BSA	Bovine serum albumin
CST	Cell Signaling Technology
PRAD	Prostate adenocarcinoma
FVB	Friend leukemia virus B susceptible mouse strain
GS	Glycogen synthase
DMSO	Dimethyl sulfoxide
CSS	Charcoal stripped serum
AKT	Protein kinase B
PKA	Protein kinase A
PKC	Protein kinase C
ILK	Integrin-linked kinase

LIST OF FIGURES

LIST OF SCHEMES

LIST OF TABLES

ACKNOWLEDGEMENTS

Firstly, I would like to acknowledge Michael Diaz for getting this project started, and Tiffany Nguyen, who will hopefully complete this project.

Lastly, I would like to acknowledge Dr. Stephanie Stanford for her support as chair and thesis advisor through the past two years. Her guidance as a teacher and mentor cannot be understated and underappreciated.

Figure 4 is coauthored with Chang, Joseph and Nguyen, Tiffany. The thesis author was the primary author of this figure.

Figure 5 is coauthored with Chang, Joseph and Diaz, Michael. The thesis author was the primary author of this figure.

ABSTRACT OF THE THESIS

Low-Molecular-Weight Protein Tyrosine Phosphatase Promotes Prostate Cancer Progression

by

Joseph Chang

Master of Science in Biology

University of California San Diego, 2019

Professor Stephanie Stanford, Chair
Professor Jens Lykke-Andersen, Co-Chair

Prostate cancer (PCa) accounts for 3.8% of cancer related deaths in males worldwide.[1] Therapeutic and surgical developments have mitigated the mortality of localized prostate cancer, yet upon the progression of the cancer to a metastatic state, the disease becomes quite lethal. New technologies and research targeting prostate cancer aim to ameliorate disease progression by inhibiting localized tumor growth or by preventing metastasis. Recent literature has reported the low-molecular-weight protein tyrosine phosphatase (LMPTP) as a protein involved in the progression of prostate cancer.[2, 3] By the complete knockout of LMPTP via CRISPR/Cas9 technology, or the inhibition of LMPTP through our recently developed orally bioavailable compound, we looked to confirm LMPTP as an oncogenic protein using systems that model prostate cancer progression. We confirmed that LMPTP confers cancer-like characteristics to prostate cancer cells *in vitro* and *in vivo*. Additionally, through molecular techniques such as Western blotting and immunofluorescence, we explored the intracellular mechanism through which LMPTP promotes cancer progression. We report a potential downstream effector of LMPTP action, and a potential axis through which this effector mediates LMPTP's oncogenic effects. In conclusion, LMPTP is a promising molecule for further phenotypic and mechanistic exploration and in the long term may reveal to be a druggable target for prostate cancer treatment.

INTRODUCTION

In nearly all biological contexts, cell signaling events are regulated by post-translational phosphorylation events, including phosphorylation on tyrosine residues. These post-translational phosphorylation events are catalyzed by protein tyrosine kinases (PTKs), whereas removal of the phosphate group is catalyzed by protein tyrosine phosphatases (PTPs). Together, the PTKs and PTPs comprise a molecular regulatory system that dynamically regulates signal transduction within the cell, thus having a large effect on key cellular processes such as survival, growth, and migration. Consequently, if dysregulated, this PTK/PTP system can contribute to various diseases and thus these enzymes are an attractive family of molecules to target in various diseases. Whereas drugs targeting PTKs have long been sought by pharmaceutical companies, only in the past decade or so have drugs targeting PTPs entered into clinical trials due to a lack of drug specificity and the consequent stigma surrounding the druggability of these PTPs.[4] However, the attitude towards targeting PTPs has been changing, and PTPs now represent a family of molecules that scientists can potentially target to treat disease.

The family of PTPs can be divided up into 3 classes: Class I is the largest subfamily of PTPs containing "classical" PTPs as well as the DUSPs, and class III contains the Cdc25 phosphatases. Class II is composed solely of our protein of interest, the low molecular weight protein tyrosine phosphatase (LMPTP).[5] LMPTP is a small 157 amino acid protein that is expressed across multiple animal kingdoms, including mammals, plants, bacteria and fungus. In humans LMPTP is ubiquitously expressed across all tissue types and biological systems. It contains the canonical PTP sequence C12X-$_5$R, where the cysteine acts as a nucleophile during catalysis. Other important amino acids are R18, which stabilizes the LMPTP-substrate complex and D129 which participates in the hydrolysis of the covalent intermediate.[6] LMPTP has been proposed to dephosphorylate transmembrane receptors such as platelet-derived growth factor receptor alpha,[7] insulin receptor[8], and ephrin-A2 receptor[9], as well as intracellular substrates such as Src[10]. LMPTP has been implicated in heart disease and failure[11], and has

been identified as a negative regulator of the IR, making it an attractive target for type 2 diabetes[8]. Additionally, several reports suggest that LMPTP is an oncoprotein in colorectal cancer[12] and prostate cancer[2].

In American men, prostate cancer is the most common type of cancer diagnosed and the second leading cause of cancer-related death.[13,14] Typically most cases of prostate cancer involve dysregulation of the androgen receptor (AR), the cellular receptor for androgens. Thus, common treatments for prostate cancer include the ablation of androgen producing organs and the blockade of androgen signaling. Physical remedies involve the complete removal of androgen producing organs such as the prostate or the testicles. Drugs against prostate cancer include abiraterone, which blocks the production of testosterone. However in most cases of prostate cancer, patients eventually progress to an androgen-independent disease state that is resistant to many of the aforementioned forms of treatment.[15] Whereas the 5-year survival for the initial diagnosis of disease is almost 100%, the 5-year survival for androgen-independent disease is only around 30%[16], with only a few effective treatments like enzalutamide, a silent antagonist that blocks the translocation of AR to the nucleus.[17] Recently, LMPTP has been reported as a prognosticator for survival in men with untreated metastatic prostate cancer, with highly expressed LMPTP correlating with shorter survival times.[2] LMPTP has also been identified as a prognostic factor for progression to a treatment resistant state, again with highly expressed LMPTP correlating with a faster time to disease-progression.[3] However, no reports are available on the role of LMPTP in prostate cancer. Additionally, while there are many reported LMPTP substrates, none have been identified in prostate cancer cells, and the mechanism of LMPTP in prostate cancer remains to be elucidated. We sought to answer questions regarding LMPTP in prostate cancer: does LMPTP promote prostate cancer growth? If so, which stages of cancer growth does LMPTP contribute to? If LMPTP is involved, how does it mediate its effect?

MATERIALS & METHODS

TCGA Analysis

Survival data for prostate adenocarcinoma (PRAD) patients was taken from ualcan.path.uab.edu, based on the Cancer Genome Atlas (TCGA) data.

Cell Culture

The Myc-CaP prostate cancer cell line (gift from Dr. Charles Sawyers) was grown in Dulbecco's minimal essential medium (DMEM) (Corning, 10-013-CV) supplemented with 10% fetal bovine serum (FBS) (Atlanta Biologicals, S1150H), 100 I.U. penicillin and 100 μg/mL streptomycin (Corning, 30-002-Cl). Androgen deprived Myc-CaP cells were grown in DMEM supplemented with 10% Charcoal/Dextran Treated FBS (Atlanta Biologicals, S11610R). Myc-CaP cells were maintained at 37°C and 5% CO_2 in a sterile incubator.

Quantitative Real-Time PCR

RNA was isolated from cells using RNeasy Plus Micro Kit (QIAGEN, 74034) according to the manufacturer's instructions. cDNA was synthesized using SuperScript III First-Strand Synthesis SuperMix (Life technologies, 11752-250) according to the manufacturer's instructions on BioRad S1000 Thermal Cycler. cDNA was diluted at 1:5 with RNase-free water. Each sample for qPCR was prepared with 0.5 μM primer, 5 μL RT^2 SYBR Green qPCR MasterMix (QIAGEN, 330503), 2.6 RNase free water, and 2 μL cDNA in a 384-well plate. qRT-PCR was performed using a BioRad CFX384 Real-Time System.

Cell Lysis and Western Blotting

Cell Lysis

Cells were lysed with Cell Lysis Buffer (Cell Signaling Technology, #9803) and 1 μM phenylmethylsulfonyl fluoride (PMSF). Lysates were scraped, collected, and sonicated for a total of 3 min and 45 sec by pulses of 15 sec separated by 45 sec. After sonication, samples were spun at max

speed at 4°C for ~30 min. Protein lysates were quantified with Pierce BCA Protein Assay Kit (Thermo, PI23227) according to the manufacturer's instructions.

Electrophoresis

Samples were prepared with 2X Laemmli SDS Sample Buffer (BioRad, 161-0737) or 6X Laemmli SDS Sample Buffer (Alfa Aesar, AAJ61337Ad) with β-mercaptoethanol. Samples were adjusted for concentration and loaded onto gel with 20-50 μg protein/well. Samples were run on a 4-20% Tris-Glycine Gel (Invitrogen, XP04200BOX) at 120 V for 1.5 hr.

Table 1. Table of antibodies used

Antibody	**Dilution**	**Company**	**Catalog Number**
Phospho-GSK-3β (Ser9) Rabbit mAb	1:1000	Cell Signaling Technology	#9336
GSK-3β (D5C5Z) XP Rabbit mAb	1:1000	Cell Signaling Technology	#12456
ACP1 α/β (Q18) Mouse mAb	1:1000	Santa Cruz Biotechnology	sc-100343
Androgen Receptor (D6F11) XP Rabbit mAb	1:1000	Cell Signaling Technology	#5153
GAPDH (14C10) Rabbit mAb	1:1000	Cell Signaling Technology	#2118
ECL Anti-Mouse IgG	1:3000	GE Healthcare	NA931
ECL Anti-Rabbit igG	1:3000	GE Healthcare	95017-556

Western Blotting

Proteins were transferred from SDS-PAGE to nitrocellulose using wet transfer method. A "sandwich" of sponges, filter paper, nitrocellulose, and the gel was prepared in transfer buffer. Transfers were

performed at 60°C for 45-90 min and membranes were blocked with 5% BSA in TBS-T for 1 hr, before probing with primary antibody in 5% BSA in TBS-T overnight. Membranes were washed 3 times with TBS-T for 10 min each before probing with secondary antibody in 5% dry milk in TBS-T for 1 hour. Membranes were washed 3 times with TBS-T for 10 min. each before addition of Immobilon Crescendo Western HRP Substrate (Millipore, WBLUR0500). Membrane was placed in HRP Substrate for 5 minutes before development using GeneSys G-Box.

Myc-CaP LMPTP knockout (KO) Generation

Plasmid Amplification & Isolation

E. coli containing plasmid pD1301-AD was purchased from ATUM. The plasmid contained a Kanamycin resistance coding sequence for bacterial selection, GFP coding sequence for mammalian cell selection, Cas9 coding sequence, and gRNA targeting the *Acp1* exon 1 locus.

gRNA sequence: 5' to 3' AGTCAGTCGTGTTCGTGTGT

E. coli were plated on agar with kanamycin. After overnight growth, a single colony was selected and grown as a starter culture in 5 mL LB medium under kanamycin selection. Starter culture was incubated for 8 hr. at 37°C and then diluted 1/1000 into 300 mL LB medium. Bacterial cultures were grown for 12 hr. at 37°C, after which the plasmids were isolated using Plasmid MaxiPrep (QIAGEN, 12162) according to the manufacturer's instructions.

Transfection

Myc-CaP cells were grown in 6-well plates. At ~65% confluence, cells were transfected with 500 ng pD1301-AD using Lipofectamine 3000 (Life Technologies, L30000015) according to the manufacturer's instructions, and processed for cell sorting after two days.

Cell Sorting

Cells were trypsinized with 0.05% trypsin (Corning, MT2505Cl) and neutralized with DMEM media. Trypsin and DMEM was removed, and the cells were washed and resuspended with FACS buffer (25

mM HEPES, 1 mM EDTA, 1% FBS in PBS). GFP positive cells were single-cell sorted (FACS-Aria) into individual wells of a 96-well plate (Corning, 3997).

Cell Culture

After 14 days, individual wells were monitored for colony formation. When a colony reached ~0.5 mm in diameter, the colony was transferred to a 24-well plate for further expansion. At ~60% confluency, each cell line was split 1:2 into two wells: one for culturing, and the other for genomic DNA (gDNA) isolation.

PCR

gDNA was isolated using DNeasy Blood and Tissue Kit (QIAGEN, 69506) according to the manufacturer's instructions. Each reaction contained 100 ng gDNA, 0.4 μM primers (total), and 2X OneTaq Master Mix (New England Biolabs, M0489S). PCR was performed using BioRad S1000 Thermal Cycler.

Primers (T_a: 58°C): Forward: 5' to 3' TCGTCCCGACGCGGTT

Reverse: 5' to 3' GCATATGAAAAAGGCAGACAAACG

The PCR products were run on 2% agarose gel with SybrSafe DNA Gel Stain (Invitrogen, S33102) at 85 V for 2 hr.

Western Blotting

Cell clones were grown in 6-well plates (Corning, 3521). Lysates were harvested and western blotting (WB) was performed according to the above procedures.

Sequencing

PCR products were purified using PCR Purification Kit (QIAGEN, 28106) according to the manufacturer's instructions. 100 ng of the purified PCR product, along with 10 μM forward and reverse primers, were sent to Eton Bioscience for Sanger sequencing. After receiving the sequences, they were analyzed using FinchTV.

Cell Proliferation Assays

Wild-type (WT) and LMPTP KO Myc-CaP lines were plated at 5,000 cells per well in 12 well plates (Falcon, 353225). Cells were allowed to grow for 5 days; media was changed on day 3. After 5 days of growth, cells were fixed with 70% ethanol for 10 minutes, then stained with 0.05% crystal violet (25% Ethanol) for 10 minutes. Afterwards, the plate was rinsed with sufficient water until no residual crystal violet was left. Plates were allowed to dry overnight, before removing crystal violet with Sorenson's Extract (50 mM sodium citrate & 50 mM citric acid). Samples were diluted 3 times with water after extraction. Diluted samples were read at an absorbance of 590 nm in triplicate using a plate reader (Infinite M1000, TECAN).

Soft Agar Assay

The bottom layer of agar was composed of a 1:1 ratio of 1.2% noble agar (VWR, 90000-772) to 2X DMEM media (Fisher, SLM-202). The bottom layer was allowed to solidify at room temperature (RT) before plating a top layer of agar composed of a 1:1 ratio of 0.6% noble agar to 2X DMEM media containing the appropriate amount of cells. WT and LMPTP KO Myc-CaP cells were plated at 35,000 cells per well in 6 well plates. This layer was allowed to solidify at RT before adding a thin layer of 1X DMEM media to keep the gel moist. Plates were placed in 37°C with 5% CO_2 for 21 days. Colonies were counted using a light microscope. Z-stacks of gels were captured using the AxioVert Marianas System and compiled using Fiji software.

***In Vivo* Xenograft Mouse Model**

200,000 WT Myc-CaP or LMPTP KO cells were suspended in a solution of 50% Matrigel Matrix Phenol Red Free (BD, #356237) and 50% DMEM cell culture media in a final volume of 100 μL. 8-week old C.B.17 SCID mice were inoculated by subcutaneous injection with the cells above the right and left hind legs. Tumors were measured with a caliper 3 times a week starting 7 days after inoculation. Mice that received compound chow were placed into separate cages 14 days after inoculation. Chow was formulated using 1% w/w Compd. 23. Tumor length, width, and depth were

measured 3 times per week using a caliper. Tumor volume was calculated by multiplying length, width, and depth. Study endpoint was reached when tumor length exceeded 2 cm or when mice lost 20% of body weight. Mice were sacrificed using a CO_2 chamber and tumors were harvested, weighed, and flash frozen in liquid nitrogen or fixed in 10% formalin. Tumors fixed in 10% formalin were transferred to 70% ethanol after 2 days.

Immunofluorescence

50,000 WT or LMPTP KO Myc-CaP cells were seeded on coverslips sterilized with 70% ethanol and UV light. After 2 days of growth, cells were fixed with 4% formaldehyde in PBS for 10 min and washed with PBS. Cells were permeabilized with 1% BSA and 0.4% Triton X-100 in PBS for 20 min at room temperature. Coverslips were incubated overnight with rabbit anti-AR antibody (CST #5153) at 1:500 dilution in 1% BSA and 0.1% Triton X-100 in PBS. Cells were washed with 1% BSA and 0.1% Triton X-100 in PBS and incubated with Alexa Fluor 488 conjugated goat anti-Rabbit IgG (Life Technologies, A11008) and washed again with PBS solution containing 1% BSA and 0.4% Triton X-100. Cells were stained with phalloidin Alexa Fluor 568 (1:100; Life Technologies, A12380) and 5 ug/mL Hoeschst 33242 (1:3000; Life Technologies, H3570). Coverslips were mounted onto slides with Prolong Gold Antifade (Life Technologies, P36934), dried overnight and imaged using a Zeiss LSM790 Confocal Microscope. Cytoplasmic AR was quantified by a phalloidin overlay; nuclear AR was quantified by a Hoechst overlay. Images were quantified using Fiji software.

RESULTS

High LMPTP expression correlates with reduced survival time of prostate adenocarcinoma (PRAD) patients

In 2006 the National Cancer Institute and the National Human Genome Research Institute participated in a cancer genomics program, the Cancer Genome Atlas (TCGA), characterizing multiple cancer types with over 20,000 total samples collected from various tissue source sites such as Memorial Sloan-Kettering Cancer Center and University of Texas MD Anderson Cancer Center. For patients with prostate adenocarcinoma, TCGA collected 500 samples, procuring large amounts of data such as mRNA expression and proteome analysis. The UALCAN database provided by the University of Alabama at Birmingham correlates TCGA data with patient outcome, allowing researchers to look at genes of interest in correlation with outcomes such as survival and disease progression.[18] Using the UALCAN database, we saw that expression of *ACP1* –the gene encoding LMPTP- significantly correlates with the survival of PRAD patients. Patients that highly express *ACP1* (as defined by being in the highest quartile of *ACP1* expression) are two times more likely to die after about 10 years with the disease **(Figure 1).** *Acp1* has also been implicated in PRAD progression, where patients highly expressing *Acp1* are two times more likely to progress to castration-resistant disease after 7.5 years.[3]

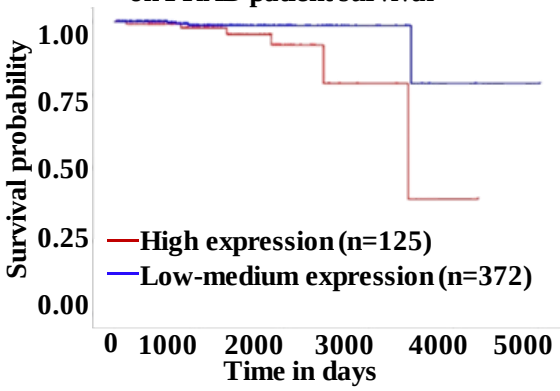

Figure 1. High LMPTP expression correlates with decreased survival time of prostate adenocarcinoma patients. Data from TCGA database (UALCAN). p=0.012

Generation of LMPTP KO Myc-CaP cells using CRISPR/Cas9 technology

Having identified *ACP1* as a potential oncogene in PRAD, we next sought to identify the role of *ACP1* in prostate cancer cells *in vitro.* We selected the Myc-CaP cell line, an androgen-independent, murine prostate cancer cell line[19], as our proof of principle model. The Myc-CaP cell line was derived through removing a large prostate carcinoma from a transgenic FVB mouse that expressed a prostate-specific *c-myc* transgene.[19] We selected the Myc-CaP cell line as an *in vitro* model since it highly expresses LMPTP and can be xenografted into immunocompromised mice. We knocked out the *Acp1* gene in these cells using CRISPR/Cas9 technology. We designed a single guide RNA targeting the Cas9 protein to exon 1 in the *Acp1* gene and single cell sorted for Myc-CaP cells that had been successfully transfected with the Cas9 plasmid, as indicated by GFP positivity (data not shown). The gDNA of single-cell clones was isolated and subjected to PCR for the region containing the possible excision. The expected PCR product was 245 bp. Clones L2, L10, L11, L12 and L14, whose amplicans appeared one or two nucleotides shorter or longer, were selected for analysis via western blot. The western blot revealed that L2, L10, and L12 were complete knockouts (KO) for LMPTP, L11 retained full LMPTP expression, and L14 displayed some residual LMPTP expression

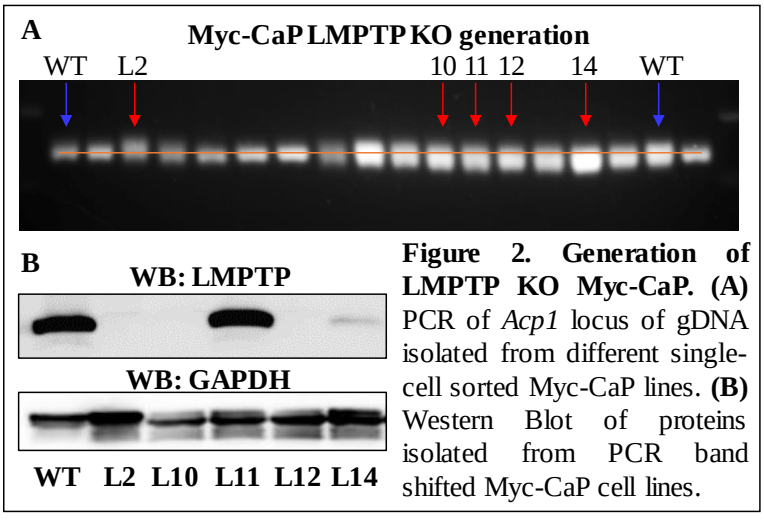

Figure 2. Generation of LMPTP KO Myc-CaP. (A) PCR of *Acp1* locus of gDNA isolated from different single-cell sorted Myc-CaP lines. **(B)** Western Blot of proteins isolated from PCR band shifted Myc-CaP cell lines.

(Figure 2). L2, L10 and L12 were selected for further experimentation and will be referred to as KO2, KO10, and KO12.

LMPTP promotes cell growth *in vitro* and *in vivo*

After we identified LMPTP KO clones, we sought to compare the growth rates of WT Myc-CaP versus our LMPTP KO Myc-CaP lines in culture. After 5 days of growth in culture in 12-well plates, KO2, KO10, and KO12 grew at about 45%, 60%, and 65%, respectively, of the rate of the WT Myc-CaP cells (**Figure 3).** We next sought to confirm LMPTP's oncogenic effects through another assay. In a soft agar colony formation assay, which models tumorigenesis of cancer cells in a 3D environment[20], LMPTP promoted a higher rate of colony formation, with the LMPTP Myc-CaP cells being about 4 times more likely to form colonies than the LMPTP KO Myc-CaP cells **(Figure 4)**. Surprisingly, the KO cells were consistently able to form larger colonies, perhaps due to the increased availability of necessary nutrients due to the decreased presence of neighboring colonies. Next, we looked to confirm the growth promoting effects of LMPTP *in vivo* in a prostate tumor xenograft model. We inoculated severe combined immunocompromised (SCID) mice with WT and KO2 Myc-CaP cells suspended in Matrigel. The tumors were scored 3 times per week. By day 7, a significant difference ($p<0.05$) between the volumes of WT and LMPTP KO tumors could be detected. The study endpoint was reached on day 30, when the first WT tumor reached 2 cm in diameter, at which point the WT tumors were more than double in size compared to the KO2 tumors **(Figure 5A).** Having confirmed that LMPTP does promote prostate cancer growth *in vivo*, we sought to understand whether the catalytic activity of LMPTP was the key driver for prostate cancer cell growth. We tested this by inoculating SCID mice with WT tumors and placing half of the mice on chow formulated with 0.1% w/w LMPTP inhibitor. The LMPTP inhibitor (Compd. 23) had been previously developed in our laboratory as an orally bioavailable compound that inhibits the catalytic activity of LMPTP[5]. Mice were placed on regular or Compd. 23 chow 14 days after inoculation. A significant difference ($p<0.05$)

was found between the tumor volumes of the mice on regular chow versus Compd. 23 chow 7 days after being placed on different chow. The first mouse with a WT tumor reached the 2 cm length experimental endpoint on day 35, when the regular chow tumors were approximately twice as large as the tumors of the mice placed on Compd. 23 chow **(Figure 5B).** Taken together these results indicate that LMPTP catalytic activity promotes prostate cancer growth *in vivo.*

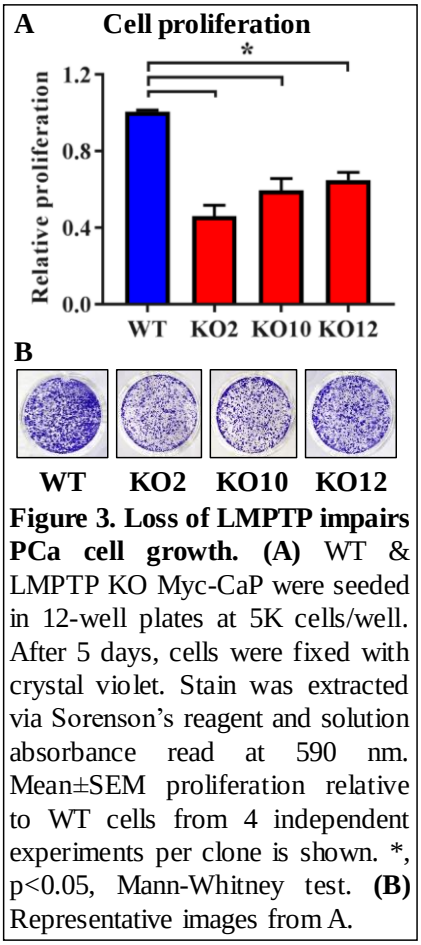

Figure 3. Loss of LMPTP impairs PCa cell growth. (A) WT & LMPTP KO Myc-CaP were seeded in 12-well plates at 5K cells/well. After 5 days, cells were fixed with crystal violet. Stain was extracted via Sorenson's reagent and solution absorbance read at 590 nm. Mean±SEM proliferation relative to WT cells from 4 independent experiments per clone is shown. *, $p<0.05$, Mann-Whitney test. **(B)** Representative images from A.

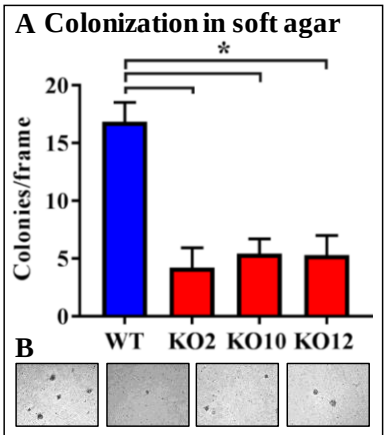

Figure 4. Loss of LMPTP inhibits tumorigenesis in PCa cells. (A) WT or LMPTP KO Myc-CaP were seeded on noble agar at 35K cells/well. After 21 days, colonies were stained with crystal violet. Mean±SEM from 4 independent experiments. *, p <0.05, Mann-Whitney test. **(B)** Representative images from A.

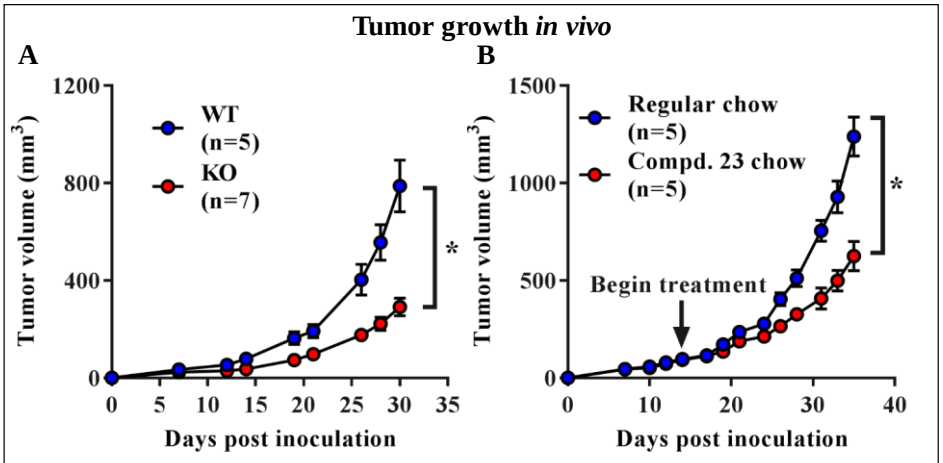

Figure 5. Inhibition of LMPTP impairs prostate tumor growth. (A) SCID mice were subcutaneously (s.c.) inoculated with 200K WT or LMPTP KO Myc-CaP cells. Tumor volumes were measured with a caliper. Mice were sacrificed when tumor length reached 2 cm. Mean±SEM % max tumor volume is shown. **(B)** Tumor volumes of mice s.c. inoculated with WT Myc-CaP cells. After 14 days, mice were placed on regular chow or chow formulated with 0.1% w/w LMPTP inhibitor Compd. 23. Mean±SEM % max tumor volume is shown. **(A, B)** *, p<0.0001, 2-way ANOVA.

LMPTP promotes GSK-3β phosphorylation on serine 9

After confirming that LMPTP promotes prostate cancer growth both *in vitro* and *in vivo*, we sought to elucidate the mechanism by which LMPTP promotes prostate cancer growth. We first compared the cell cycles of the WT and KO Myc-CaP cell lines by propidium iodide staining via FACS and did not find any differences (data not shown). Next, we looked at apoptosis of the cells by Annexin V staining via FACS and also did not find any differences between the WT and the KO cell lines (data not shown). Not finding any phenotypic differences via FACS that affect cancer growth and survival, we turned to looking at the phosphorylation of signaling pathways that LMPTP is known to affect. It has been previously reported that the LMPTP is a negative regulator of insulin signaling by dephosphorylating the insulin receptor directly[8], so we started by looking at the phosphorylation of molecules in the insulin signaling pathway. Insulin receptor tyrosine phosphorylation, and AKT serine and threonine phosphorylation were unaffected in the LMPTP KO cells compared to the WT cells (data not shown). However, when we looked at GSK-3β phosphorylation, a known substrate of AKT, we saw that LMPTP-expressing Myc-CaP cells displayed more phosphorylation on the serine 9 site of GSK-3β. **(Figure 6)** The phosphorylation site of serine 9 is an inhibitory phosphorylation site in GSK-3β[21], thus when LMPTP is present in Myc-CaP, GSK-3β is more inhibited and inactive than in LMPTP KO cells.

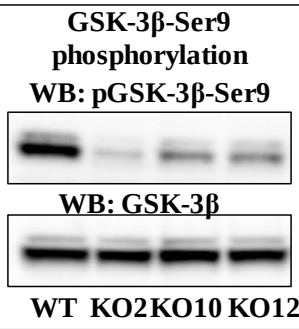

Figure 6. LMPTP KO reduces GSK-3β Ser9 phosphorylation. GSK-3β phosphorylation was assessed in wild-type (WT) and LMPTP Myc-CaP by Western blotting (WB). Representative of 3 independent experiments for lines 2 and 12 and two independent experiments for line 10.

LMPTP promotes androgen receptor translocation into the nucleus

Having identified that LMPTP leads to more GSK-3β serine 9 phosphorylation and thus GSK-3β inhibition, we sought to identify how an inhibited GSK-3β can lead to increased prostate cancer growth. GSK-3β is a known kinase of glycogen synthase (GS) which when phosphorylated on serine 641 results in GS inactivation leading to the inhibition of glycogen production.[22,23] Cancer cells are known to rely heavily on glycogen for energy since tumors grow in a hypoxic microenvironment.[24] According to our hypothesis, the inactive GSK-3β would not phosphorylate GS, resulting in an active GS that enables the cell to proliferate even under hypoxic conditions. We looked at GS phosphorylation on serine 641 via WB but found no difference in phosphorylation (data not shown). Additionally, GSK-3β is also a known regulator of β-catenin degradation. Phosphorylation of β-catenin by GSK-3β would lead to the destruction of β-catenin through subsequent ubiquitination and destruction via E3-ligase.[25] In WT cells, the GSK-3β is less active than in LMPTP KO cells, allowing more β-catenin to remain in the cell, potentially leading to an increase of β-catenin regulated oncogenes.[26] When we examined β-catenin expression, we saw no differences between the WT and KO Myc-CaP cells (data not shown). Next, we turned our attention to the androgen receptor (AR). The AR is also reported to be phosphorylated by GSK-3β, potentially preventing AR translocation to the nucleus.[27] In LMPTP-expressing cells, the inactive GSK-3β would lead to decreased AR phosphorylation, leading to increased translocation of AR to the nucleus and a corresponding expression of androgen response elements, genes critical to the growth of prostate cancer cells. Before looking at AR translocation to the nucleus, we confirmed that AR expression was not different between WT and KO Myc-CaP cells **(Figure 7)**. Using immunofluorescence to look at AR translocation, we saw that AR was predominantly located in the nucleus in WT Myc-CaP cells, whereas some AR of the KO Myc-CaP cells was localized to the cytoplasm. By staining the nucleus with Hoechst and the cytoskeleton with phalloidin, we were able to quantify the ratio of nuclear to cytoplasmic AR using Fiji software. The ratio of cytoplasmic to nuclear AR in WT Myc-CaP cells was

0.337 whereas the ratio of cytoplasmic to nuclear in KO2, KO10, KO12 Myc-CaP cells was 0.5837, 0.4692, 0.4350 respectively, suggesting that more AR in KO cells remained in the cytoplasm compared to the WT cells **(Figure 8A)**. We also sought to confirm that the catalytic activity of LMPTP was necessary for AR translocation; therefore we performed the same experiment with WT Myc-CaP cells in the presence of DMSO and Compd. AR nuclear translocation. AR in cells treated with DMSO existed at a cytoplasmic to nuclear ratio of 0.319, whereas AR in cells treated with Compd. 23 displayed a cytoplasmic to nuclear ratio of 0.5383 **(Figure 8B)**.

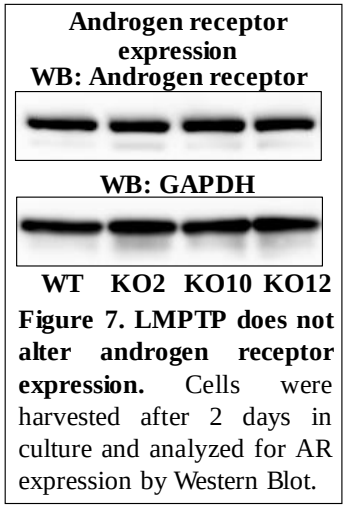

Figure 7. LMPTP does not alter androgen receptor expression. Cells were harvested after 2 days in culture and analyzed for AR expression by Western Blot.

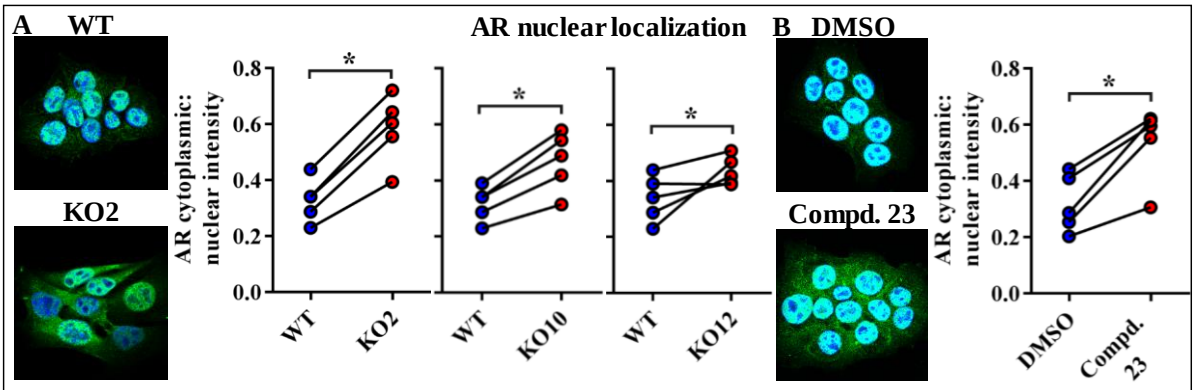

Figure 8. LMPTP promotes androgen receptor (AR) nuclear localization. WT or LMPTP KO Myc-CaP were seeded at 50k/well. After 2 d, cells were fixed with 4% PFA, and permeabilized with 0.4% Triton X-100. Cells were stained with anti-AR Ab, goat anti-rabbit Alexa Fluor 488 Ab, Phalloidin 568 and Hoechst. **(A)** WT and LMPTP KO Myc-CaP. **(B)** WT Myc-CaP treated with DMSO or 10 μM Compd. 23 for 18 hr. **(A-B)** Mean±SEM from 5 independent experiments. *, $p<0.05$; Mann-Whitney test.

LMPTP promotes transcription of androgen response elements

We sought to confirm LMPTP's anti-nuclear effect on AR through a secondary method. To do this, we looked at mRNA expression of *Fkbp5* via qPCR. *Fkbp5* encodes a FK506 binding protein, a co-chaperone that acts with Hsp90.[28] *Fkbp5* is also under the control of an AR-regulated promoter, making it a common measure of AR transcriptional activity. By qPCR we observed a ~25% decrease of *Fkbp5* expression in each of the LMPTP KO Myc-CaP lines, confirming a decrease in AR transcriptional activity in LMPTP absent cells **(Figure 9)**. Taken together, our results suggest that LMPTP may promote prostate cancer cell growth by increasing GSK-3β serine 9 phosphorylation, which in turn promotes the transcriptional activity of AR.

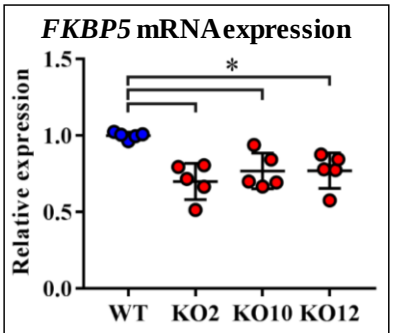

Figure 9. Loss of LMPTP inhibits transcription of AR-dependent gene. *FKBP5* expression was analyzed in WT and LMPTP KO Myc-CaP by qPCR. Mean±SEM *FKBP5* expression after normalization to *GAPDH* from 5 independent experiments. *, $p<0.05$; Mann-Whitney test.

LMPTP promotes AR translocation to the nucleus in an androgen-independent manner

Prostate cancer is most lethal to patients when the disease progresses to an androgen-independent state where the AR is transcriptionally active even in the absence of androgen. To test whether LMPTP acts in an androgen-dependent or –independent manner, we grew cells in the

presence of charcoal-stripped serum (CSS), which had been depleted of androgens, and analyzed the cells in a similar manner, using immunofluorescence as described previously. As expected, more AR was located in the cytoplasm in CSS conditions, but the ratio of cytoplasmic:nuclear AR was still around 0.7511 in the WT cells indicating that some AR translocates to the nucleus independently of androgen in Myc-CaP cells. When comparing the ratio of cytoplasmic:nuclear AR of the WT versus the KO, there were some androgen-independent effects of LMPTP on AR, however only one of the KO cell-lines showed a significant difference with a ratio of 0.8947 compared to the WT of 0.7511 **(Figure 10)**.

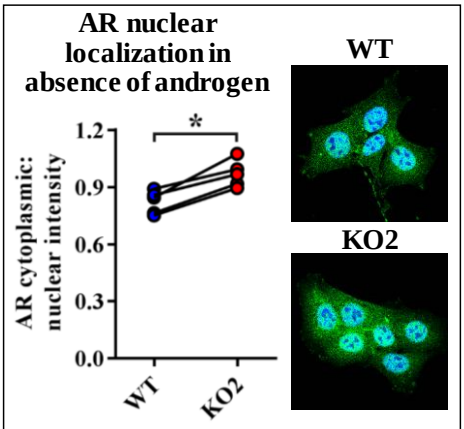

Figure 10. LMPTP promotes AR nuclear localization in an androgen-independent manner. WT or LMPTP KO Myc-CaP were seeded at 60k/well in media containing 10% charcoal-stripped serum. Cells were fixed, permeabilized and stained as in **Fig. 6.** Mean±SEM from 5 independent experiments. *, $p<0.001$; Mann-Whitney test.

DISCUSSION

Using the Myc-CaP murine cell model both *in vitro* and *in vivo* we present data implicating LMPTP as a driver of prostate cancer carcinogenesis. LMPTP has been linked to different facets of disease progression in prostate cancer, including metastasis[2] and progression to castration-resistant disease[16]. Using different *in vitro* assays, we have confirmed that LMPTP also promotes tumorigenesis and proliferative growth, two hallmarks of cancer. These results *in vitro* were confirmed *in vivo*, where tumors without LMPTP activity grew slower in mice. Altogether, these findings suggest that LMPTP has an important role in the establishment and growth of prostate cancer.

In other phenotypic studies comparing cancerous vs. normal prostate, it has been identified that overexpression of LMPTP upregulates pathways correlating with cell migration, resistance to anoikis, and decreased adherence[29], suggesting that LMPTP could impoart a metastatic phenotype in prostate cancer. This is of note since bone metastases are a leading cause of PCa related patient death.[30] We will probe LMPTP's role in bone metastasis in future studies using both *in vitro* and *in vivo* assays. Prostate cancer cells must progress through distinct steps to become a full-fledged metastasis, so we are performing different experiments that model the different steps of bone metastasis. First, we will be injecting WT and LMPTP KO Myc-CaP cells into the tibia of mice to look at the ability of PCa cells with or without LMPTP to colonize the bone, representing the first step of metastasis. Second, our collaborators using our CRISPR/Cas9 generated C4-2B LMPTP KO cells will be looking at their ability to travel through a layer of biomaterial that mimics the bone microenvironment. We expect to observe cells without LMPTP having an impaired and compromised ability to metastasize at all stages.

At the molecular level, through various proteomic and cellular assays, we have identified two molecules through which LMPTP may act to induce prostate cancer progression. The first, GSK-3β, a kinase with numerous substrates, displays a marked decrease of phosphorylation on inhibitory

phosphorylation site serine 9 in LMPTP KO cells. We also saw no differential phosphorylation of AKT, a kinase that phosphorylates GSK-3β. Taken together, this suggests that LMPTP is an upstream regulator of GSK-3β, independent of the AKT pathway. LMPTP may regulate GSK-3β through a number of direct upstream regulators of GSK-3β, such as PKA, PKC, p90RSK, and ILK. We will be looking for differential expression or differential activity in these molecules listed, and other potential upstream substrates by WB or immunoprecipitation in order to fully understand how LMPTP mediates its GSK-3β inhibiting activity **(Scheme 1)**. The second molecule, AR, is a cytoplasmic receptor protein that acts as a transcription factor in response to androgen to express prostate cancer promoting genes. We find that cells lacking the catalytic activity of LMPTP whether by complete KO or chemical inhibition display reduced AR translocation into the nucleus. This may be mediated through GSK-3β

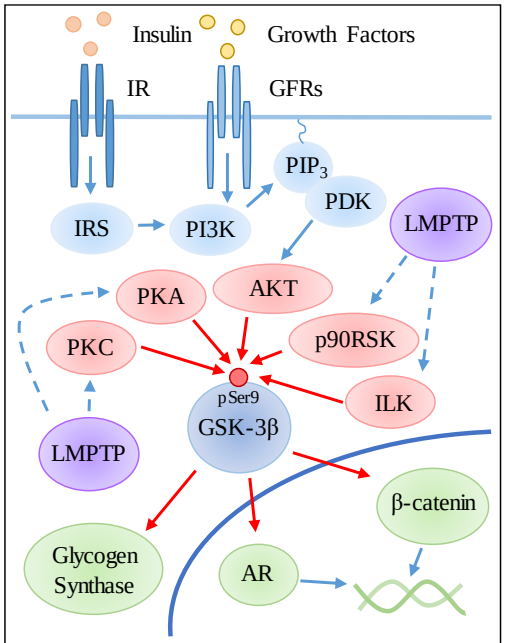

Scheme 1. Scheme depicting LMPTP-promoted PCa cell growth through GSK-3β inhibition. Activating signals shown in blue, inhibitory signals shown in red. Models depicting potential inhibitory modes of action of GSK-3β are shown in green. GFRs, growth factor receptors; IRS, insulin receptor substrate; PIP_3, phosphatidylinositol (3,4,5) triphosphate; PDK, phosphoinositide-dependent kinase.

which has been reported to prevent AR translocation[25], or through another LMPTP-affected pathway or molecule. Experiments are currently ongoing to determine whether the effect of LMPTP on AR is independent of or dependent on GSK-3β.

Furthermore, we have evidence that LMPTP may mediate its effect on AR in an androgen-independent manner. In the current climate of prostate cancer, patients have nearly a 100% survival rate for localized or regional disease that is still androgen-dependent.[13,14] This high survival rate is due to an improved ability to detect disease earlier, as well as the development of various treatments primarily targeting androgen-dependent AR activity, known as androgen deprivation therapy. Some of these treatments involve physical castration, the removal of androgen-producing organs such as radical prostatectomy or orchiectomy, while other treatments involve chemical castration, chemically blocking the activity of AR using a drug, such as abiraterone. However, patients who have been treated with these anti-androgen treatments often progress to a disease state that acts independently of androgen activity, with either overexpressed or constitutively active AR. This advanced disease state is known as androgen-independent or castration resistant prostate cancer. Prostate cancer patients who have progressed to androgen-independent or castration resistant disease have a dramatically decreased survival rate of 28%.[13,14] By showing that LMPTP can act on AR in an androgen free setting, we have demonstrated that LMPTP may induce its effect on AR in both androgen-dependent and –independent disease.

A few decades ago in oncology, phosphatases were largely considered to be tumor suppressors as the opposites to oncogenic kinases. This, combined with the high intrasimilarity of phosphatases relative to kinases, made phosphatases an unattractive drug target. However, research in the last decade or so has implicated many different phosphatases as oncogenes in many different cancers such as colorectal, lung, breast and gastric cancers. As other tyrosine phosphatases such as SHP2 have entered the field as attractive drug targets, we have identified LMPTP as another potential tyrosine

phosphatase to target. While much remains to be done in identifying the substrate and elucidating the signaling pathways affected by LMPTP, by showing that LMPTP is crucial to AR activity, we demonstrate LMPTP is another molecule to potentially target for prostate cancer therapy. In conclusion, we demonstrate that LMPTP contributes to the overall progression of prostate cancer and promotes activation of the androgen receptor in prostate cancer cells.

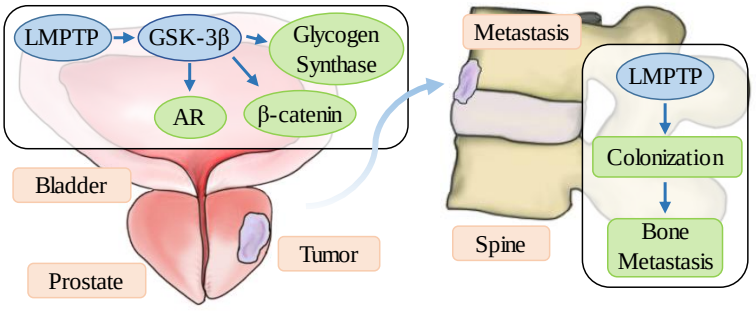

Scheme 2. Scheme depicting prostate tumor growth and bone metastasis. Activating signals shown in blue. Model depicting potential modes of action of GSK-3β are shown in left. Model depicting potential effect of LMPTP on bone metastasis shown in right.

BIBLIOGRAPHY

1 Rawla, P. Epidemiology of Prostate Cancer. *World J Oncol* **10**, 63-89, doi:10.14740/wjon1191 (2019).

2 Ruela-de-Sousa, R. R., Hoekstra, E., Hoogland, A. M., Souza Queiroz, K. C., Peppelenbosch, M. P., Stubbs, A. P., Pelizzaro-Rocha, K., van Leenders, G., Jenster, G., Aoyama, H., Ferreira, C. V. & Fuhler, G. M. Low-Molecular-Weight Protein Tyrosine Phosphatase Predicts Prostate Cancer Outcome by Increasing the Metastatic Potential. *Eur Urol* **69**, 710-719, doi:10.1016/j.eururo.2015.06.040 (2016).

3 Miyoshi, Y., Ohtaka, M., Kawahara, T., Ohtake, S., Yasui, M., Uemura, K., Yoneyama, S., Yokomizo, Y., Uemura, H., Miyamoto, H. & Yao, M. Prediction of Time to Castration-Resistant Prostate Cancer Using Low-Molecular-Weight Protein Tyrosine Phosphatase Expression for Men with Metastatic Hormone-Naive Prostate Cancer. *Urol Int* **102**, 37-42, doi:10.1159/000493324 (2019).

4 Stanford, S. M. & Bottini, N. Targeting Tyrosine Phosphatases: Time to End the Stigma. *Trends Pharmacol Sci* **38**, 524-540, doi:10.1016/j.tips.2017.03.004 (2017).

5 Alonso, A., Sasin, J., Bottini, N., Friedberg, I., Friedberg, I., Osterman, A., Godzik, A., Hunter, T., Dixon, J. & Mustelin, T. Protein tyrosine phosphatases in the human genome. *Cell* **117**, 699-711, doi:10.1016/j.cell.2004.05.018 (2004).

6 Caselli, A., Paoli, P., Santi, A., Mugnaioni, C., Toti, A., Camici, G. & Cirri, P. Low molecular weight protein tyrosine phosphatase: Multifaceted functions of an evolutionarily conserved enzyme. *Biochim Biophys Acta* **1864**, 1339-1355, doi:10.1016/j.bbapap.2016.07.001 (2016).

7 Chiarugi, P., Cirri, P., Raugei, G., Manao, G., Taddei, L. & Ramponi, G. Low M(r) phosphotyrosine protein phosphatase interacts with the PDGF receptor directly via its catalytic site. *Biochem Biophys Res Commun* **219**, 21-25, doi:10.1006/bbrc.1996.0174 (1996).

8 Stanford, S. M., Aleshin, A. E., Zhang, V., Ardecky, R. J., Hedrick, M. P., Zou, J., Ganji, S. R., Bliss, M. R., Yamamoto, F., Bobkov, A. A., Kiselar, J., Liu, Y., Cadwell, G. W., Khare, S., Yu, J., Barquilla, A., Chung, T. D. Y., Mustelin, T., Schenk, S., Bankston, L. A., Liddington, R. C., Pinkerton, A. B. & Bottini, N. Diabetes reversal by inhibition of the low-molecular-weight tyrosine phosphatase. *Nat Chem Biol* **13**, 624-632, doi:10.1038/nchembio.2344 (2017).

9 Locard-Paulet, M., Lim, L., Veluscek, G., McMahon, K., Sinclair, J., van Weverwijk, A., Worboys, J. D., Yuan, Y., Isacke, C. M. & Jorgensen, C. Phosphoproteomic analysis of interacting tumor and endothelial cells identifies regulatory mechanisms of transendothelial migration. *Sci Signal* **9**, ra15, doi:10.1126/scisignal.aac5820 (2016).

10 Zambuzzi, W. F., Granjeiro, J. M., Parikh, K., Yuvaraj, S., Peppelenbosch, M. P. & Ferreira, C. V. Modulation of Src activity by low molecular weight protein tyrosine phosphatase during osteoblast differentiation. *Cell Physiol Biochem* **22**, 497-506, doi:10.1159/000185506 (2008).

11 Wade, F., Quijada, P., Al-Haffar, K. M., Awad, S. M., Kunhi, M., Toko, H., Marashly, Q., Belhaj, K., Zahid, I., Al-Mohanna, F., Stanford, S. M., Alvarez, R., Liu, Y., Colak, D., Jordan,

M. C., Roos, K. P., Assiri, A., Al-Habeeb, W., Sussman, M., Bottini, N. & Poizat, C. Deletion of low molecular weight protein tyrosine phosphatase (Acp1) protects against stress-induced cardiomyopathy. *J Pathol* **237**, 482-494, doi:10.1002/path.4594 (2015).

12 Hoekstra, E., Kodach, L. L., Das, A. M., Ruela-de-Sousa, R. R., Ferreira, C. V., Hardwick, J. C., van der Woude, C. J., Peppelenbosch, M. P., Ten Hagen, T. L. & Fuhler, G. M. Low molecular weight protein tyrosine phosphatase (LMWPTP) upregulation mediates malignant potential in colorectal cancer. *Oncotarget* **6**, 8300-8312, doi:10.18632/oncotarget.3224 (2015).

13 Bashir, M. N. Epidemiology of Prostate Cancer. *Asian Pac J Cancer Prev* **16**, 5137-5141, doi:10.7314/apjcp.2015.16.13.5137 (2015).

14 Siegel, R. L., Miller, K. D. & Jemal, A. Cancer statistics, 2019. *CA Cancer J Clin* **69**, 7-34, doi:10.3322/caac.21551 (2019).

15 Tran, K. & McCormack, S. in *Androgen Receptor Targeted Agents for Castration Resistant Prostate Cancer: A Review of Clinical Effectiveness and Cost-Effectiveness CADTH Rapid Response Reports* (2019).

16 Kirby, M., Hirst, C. & Crawford, E. D. Characterising the castration-resistant prostate cancer population: a systematic review. *Int J Clin Pract* **65**, 1180-1192, doi:10.1111/j.1742-1241.2011.02799.x (2011).

17 Saad, F. Evidence for the efficacy of enzalutamide in postchemotherapy metastatic castrate-resistant prostate cancer. *Ther Adv Urol* **5**, 201-210, doi:10.1177/1756287213490054 (2013).

18 Chandrashekar, D. S., Bashel, B., Balasubramanya, S. A. H., Creighton, C. J., Ponce-Rodriguez, I., Chakravarthi, B. & Varambally, S. UALCAN: A Portal for Facilitating Tumor Subgroup Gene Expression and Survival Analyses. *Neoplasia* **19**, 649-658, doi:10.1016/j.neo.2017.05.002 (2017).

19 Watson, P. A., Ellwood-Yen, K., King, J. C., Wongvipat, J., Lebeau, M. M. & Sawyers, C. L. Context-dependent hormone-refractory progression revealed through characterization of a novel murine prostate cancer cell line. *Cancer Res* **65**, 11565-11571, doi:10.1158/0008-5472.CAN-05-3441 (2005).

20 Borowicz, S., Van Scoyk, M., Avasarala, S., Karuppusamy Rathinam, M. K., Tauler, J., Bikkavilli, R. K. & Winn, R. A. The soft agar colony formation assay. *J Vis Exp*, e51998, doi:10.3791/51998 (2014).

21 Beurel, E., Grieco, S. F. & Jope, R. S. Glycogen synthase kinase-3 (GSK3): regulation, actions, and diseases. *Pharmacol Ther* **148**, 114-131, doi:10.1016/j.pharmthera.2014.11.016 (2015).

22 Orena, S. J., Torchia, A. J. & Garofalo, R. S. Inhibition of glycogen-synthase kinase 3 stimulates glycogen synthase and glucose transport by distinct mechanisms in 3T3-L1 adipocytes. *J Biol Chem* **275**, 15765-15772, doi:10.1074/jbc.M910002199 (2000).

23 Mora, A., Sakamoto, K., McManus, E. J. & Alessi, D. R. Role of the PDK1-PKB-GSK3 pathway in regulating glycogen synthase and glucose uptake in the heart. *FEBS Lett* **579**, 3632-3638, doi:10.1016/j.febslet.2005.05.040 (2005).

24 Pelletier, J., Bellot, G., Gounon, P., Lacas-Gervais, S., Pouyssegur, J. & Mazure, N. M. Glycogen Synthesis is Induced in Hypoxia by the Hypoxia-Inducible Factor and Promotes Cancer Cell Survival. *Front Oncol* **2**, 18, doi:10.3389/fonc.2012.00018 (2012).

25 Wu, D. & Pan, W. GSK3: a multifaceted kinase in Wnt signaling. *Trends Biochem Sci* **35**, 161-168, doi:10.1016/j.tibs.2009.10.002 (2010).

26 Shtutman, M., Zhurinsky, J., Simcha, I., Albanese, C., D'Amico, M., Pestell, R. & Ben-Ze'ev, A. The cyclin D1 gene is a target of the beta-catenin/LEF-1 pathway. *Proc Natl Acad Sci U S A* **96**, 5522-5527, doi:10.1073/pnas.96.10.5522 (1999).

27 Salas, T. R., Kim, J., Vakar-Lopez, F., Sabichi, A. L., Troncoso, P., Jenster, G., Kikuchi, A., Chen, S. Y., Shemshedini, L., Suraokar, M., Logothetis, C. J., DiGiovanni, J., Lippman, S. M. & Menter, D. G. Glycogen synthase kinase-3 beta is involved in the phosphorylation and suppression of androgen receptor activity. *J Biol Chem* **279**, 19191-19200, doi:10.1074/jbc.M309560200 (2004).

28 Fries, G. R., Gassen, N. C. & Rein, T. The FKBP51 Glucocorticoid Receptor Co-Chaperone: Regulation, Function, and Implications in Health and Disease. *Int J Mol Sci* **18**, doi:10.3390/ijms18122614 (2017).

29 Taitt, H. E. Global Trends and Prostate Cancer: A Review of Incidence, Detection, and Mortality as Influenced by Race, Ethnicity, and Geographic Location. *Am J Mens Health* **12**, 1807-1823, doi:10.1177/1557988318798279 (2018).

30 Jin, J. K., Dayyani, F. & Gallick, G. E. Steps in prostate cancer progression that lead to bone metastasis. *Int J Cancer* **128**, 2545-2561, doi:10.1002/ijc.26024 (2011).